

Analysis and Design of Optical Demultiplexer Based on Arrayed Plasmonic Slot Cavities: Transmission Line Model

Meisam Bahadori, Ali Eshaghian, Hossein Hodaei, Mohsen Rezaei, and Khashayar Mehrany

Abstract—A simple yet accurate model for the analysis of coupling between arrayed plasmonic slot cavities and bus/drop metal-dielectric-metal waveguides is presented. The evanescent coupling region is replaced by a transmission line section whose propagation constant and characteristic impedance are given in closed form. The side coupling between the bus waveguide and the slot cavity is modeled together with the direct coupling between the slot cavity and the drop channel. The proposed model is validated by using rigorous numerical method, and is used to design a typical demultiplexer.

Index Terms—Demultiplexing, optical filters, plasmons.

I. INTRODUCTION

ON ACCOUNT of the Wavelength Division Multiplexing (WDM) popularity in telecommunications, optical add/drop multiplexer/demultiplexers are amongst the highly in demand photonic devices. It is therefore no wonder that much effort has recently been devoted to the development of surface-plasmon-based multiplexers and routers. Evidently, the particular interest in using surface plasmons is driven by the imperatives of nanoscale integration. Although different geometrical arrangements have been exploited to realize surface-plasmon-based multiplexing, demultiplexing, and routing of optical signals [1], the schemes based on planar nano-structures are preferable because they do not need precise control over nanoparticles or any other non-planar nano-structures. Notably, an ultra-compact wavelength demultiplexer has been recently proposed by using arrayed plasmonic slot cavities [2]. It provides three major benefits. First, the center wavelength of each channel can be controlled by finding the proper length for the slot cavity that selects the demultiplexed wavelength. Second, the bandwidth of the channel can be adjusted by manipulation of the coupling efficiency between the slot cavity and the bus/drop waveguide. Third, single band transmission for each channel can be guaranteed by choosing the proper position for the drop waveguide [2]. Unfortunately, none of the abovementioned benefits is efficiently materialized if the geometrical dimensions of the demultiplexer are to be extracted by using a brute-force numerical method. Therefore,

a simple but accurate enough model for the analysis and design of arrayed plasmonic slot cavities is highly desirable.

It is the aim of this letter to propose a transmission line model to rapidly yet accurately obtain the transmission spectra of the arrayed plasmonic slot cavity demultiplexer. Thanks to the similarity between the TEM mode supported by the standard parallel-plate waveguide and the fundamental plasmonic mode of the metal-dielectric-metal (MDM) waveguides [3], miscellaneous planar plasmonic circuits based on the MDM arrangement have been successfully analyzed [3]–[6]. Still no such model has ever been proposed for arrayed plasmonic slot cavities. Since evanescent coupling plays the major role in the operation of arrayed plasmonic slot cavities, the to-be-proposed transmission line model should address the evanescent coupling mechanism. The easiest way to do this is to employ the temporal coupled mode theory [7]. But not only the incorporation of the temporal coupled mode theory in transmission line theory is itself a problematic issue; also the calculation of coupling coefficients incurs some computational burden and complicates the model. Therefore, purely analytic transmission line model is preferred. The first attempt toward such modeling has been recently reported by resorting to the spatial coupled mode theory [8], which is simpler than the temporal one. Here, we propose a new methodology and replace the coupling region by an appropriate transmission line section. In this way, the necessity of coupling coefficient calculation is eliminated altogether.

II. ANALYSIS AND DESIGN APPROACH

First, the direct coupling via evanescent wave tunneling between two codirectional MDM waveguides [see Fig. 1(a)] is examined. Second, the side coupling between two perpendicular MDM waveguides [see Fig. 2(a)] is studied. The former is then used to model the direct coupling between the slot cavities and the drop channels while the latter is employed to model the side coupling between the bus waveguides and the slot cavities. In this letter, the dielectric and metallic regions are assumed to be air and silver. The permittivity of silver is approximated by the well-known Drude model [2].

The proposed transmission line model for the direct coupling in the structure of Fig. 1(a) is shown in Fig. 1(b). The transmission line model for MDM waveguides is already available [3]–[5] but the metallic gap between the direct coupled MDM waveguides remains to be modeled. A lossy transmission line section of length d can model the metallic gap whenever diffraction at the end of the MDM waveguide

Manuscript received January 30, 2013; revised February 20, 2013; accepted February 27, 2013. Date of publication March 7, 2013; date of current version March 29, 2013.

The authors are with the Sharif University of Technology, Tehran 11365-8639, Iran (e-mail: meisambahadori@gmail.com; eshaghian@ee.sharif.ir; hhodaei@ee.sharif.ir; mrezaei86@ee.sharif.ir; mehrany@sharif.edu).

Color versions of one or more of the figures in this letter are available online at <http://ieeexplore.ieee.org>.

Digital Object Identifier 10.1109/LPT.2013.2250951

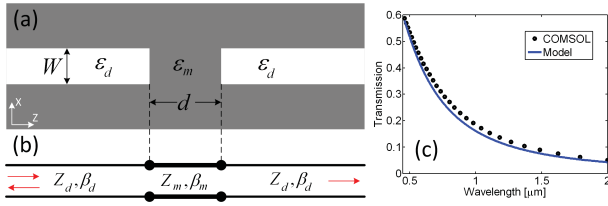


Fig. 1. (a) Direct coupling between two codirectional MDM waveguides. (b) Corresponding transmission line model. (c) Coupling efficiency of the direct-coupled structure.

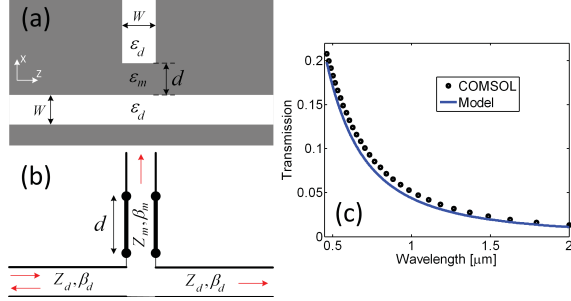


Fig. 2. (a) Side coupling between two perpendicular MDM waveguides. (b) Corresponding transmission line model. (c) Coupling efficiency of the side-coupled arrangement.

is negligible. This is usually the case when the gap is small. Furthermore, if the incoming wave is highly confined, e.g. when W is small, the propagation constant of the transmission line representing the metallic gap; β_m , can be approximated by the phase matching condition at the interface between the end of the MDM waveguide and the metallic gap:

$$\beta_m = \sqrt{\beta_d^2 + k_0^2(\epsilon_m - \epsilon_d)} \quad (1)$$

where k_0 , β_d , ϵ_m and ϵ_d are the vacuum wave-number, propagation constant of the MDM waveguide, metal and dielectric permittivity. This expression guarantees the continuity of the transverse electromagnetic fields at the intersection between the metallic gap and the dielectric region, wherein the incoming wave is confined. Much like the transmission line model for MDM waveguides whose characteristic impedance; Z_d , can be written in terms of β_d , ϵ_d and angular frequency ω [3], the characteristic impedance of the gap; Z_m , can be written as:

$$Z_{d,m} = W\beta_{d,m}/(\omega\epsilon_0\epsilon_{d,m}). \quad (2)$$

The reflection coefficient of the direct-coupled structure is then obtained as:

$$R_D = (Z_{in} - Z_d)/(Z_{in} + Z_d) \quad (3)$$

where Z_{in} is the input impedance seen at the input of the lossy transmission line:

$$Z_{in} = Z_m(Z_d + jZ_m \tan(\beta_m d))/(Z_m + jZ_d \tan(\beta_m d)). \quad (4)$$

The coupling efficiency through the metallic gap is then:

$$T_D = (1 + R_D) \cos(\beta_m d) - j(1 - R_D) \sin(\beta_m d) Z_m / Z_d. \quad (5)$$

Fig. 1(c) demonstrates the accuracy of the abovementioned expression for a typical direct-coupled structure with geometrical parameters $W = 50$ nm, and $d = 10$ nm.

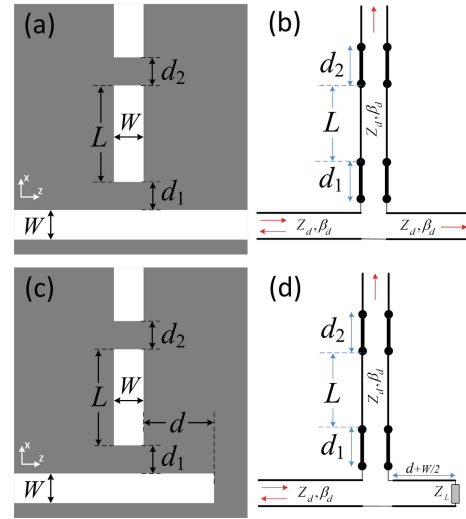


Fig. 3. (a) Single channel demultiplexer and (b) its corresponding model. (c) Single channel demultiplexer with a terminated bus and (d) its corresponding transmission line model.

The side-coupling between two perpendicular MDM waveguides in Fig. 2(a) can be modeled similarly. The evanescent coupling region should be replaced by the same transmission line but in a new configuration. This new configuration shown in Fig. 2(b) conforms to the geometrical arrangement of the side-coupled waveguides. The input impedance of the lossy transmission line is again equal to the one presented in Eq.(4) and therefore, the reflection coefficient at the input port is:

$$R_S = Z_{in}/(Z_{in} + 2Z_d). \quad (6)$$

The transmission coefficient (coupling efficiency) through the metallic gap in this configuration is then

$$T_S = 2R_S \cos(\beta_m d) - j(1 - R_S) \sin(\beta_m d) Z_m / Z_d \quad (7)$$

and its accuracy for a structure with $W = 50$ nm and $d = 10$ nm is demonstrated in Fig. 2(c).

Given that wavelength demultiplexing in arrayed plasmonic slot couplers is owed to the side- and direct-coupling between the slot cavity and the bus waveguide/drop channels, the proposed transmission line models can replace the time-consuming brute-force numerical methods in analysis and design of $1 \times N$ arrayed plasmonic slot cavity demultiplexers. To demonstrate this, a single channel demultiplexer is considered first. This structure is shown together with its corresponding transmission line model in Fig. 3(a) and (b), respectively. The slot cavity is in fact an MDM waveguide terminated at its both ends. It is therefore represented by the transmission line model of the MDM waveguide sandwiched between the metallic gap transmission lines. The transmission coefficient from the bus waveguide to the drop channel is calculated as:

$$\begin{aligned} T = & [\cos(\beta_m d_2) \cos(\beta_d L) - \sin(\beta_m d_2) \sin(\beta_d L) Z_m / Z_d] \\ & \times [2R \cos(\beta_m d_1) - j(1 - R) \sin(\beta_m d_1) Z_m / Z_d] \\ & - [\sin(\beta_m d_2) \cos(\beta_d L) + \cos(\beta_m d_2) \sin(\beta_d L) Z_d / Z_m] \\ & \times [2R \sin(\beta_m d_1) + j(1 - R) \cos(\beta_m d_1) Z_m / Z_d] \quad (8) \end{aligned}$$

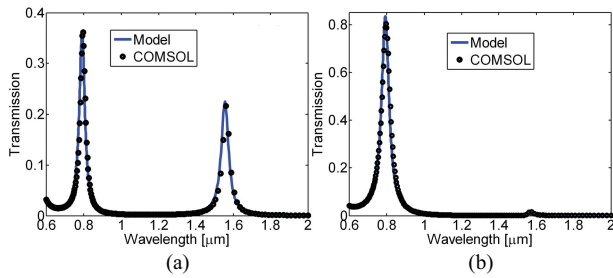


Fig. 4. Transmitted power spectrum of the single channel demultiplexer. (a) Nonterminated bus waveguide. (b) Terminated bus waveguide.

where R is the reflection coefficient at the input port of the bus. It can be easily obtained in terms of the input impedance of the channel [see Eq.(6)].

The slot cavity selects the resonant wavelength of the incoming wave in the bus waveguide and opens several windows in the transmission spectrum of the drop channel. This is shown in Fig. 4(a), where the transmitted power in the drop channel of a typical structure with $W = 50$ nm, $d_1 = 10$ nm, $d_2 = 10$ nm, and $L = 505$ nm is plotted versus wavelength. There is an excellent agreement between the results obtained by the proposed transmission line model (solid line) and those obtained by the COMSOL software (circles). The proposed model can then be used to find the appropriate geometrical dimensions of the structure needed to have the desired resonant wavelength and bandwidth for the channel. Still, there are two major obstacles to overcome. First, single band transmission is not guaranteed. Second, the transmission efficiency is as low as 36% because there is a high impedance mismatch at the input of the drop channel. It is fortunately possible to resolve both these problems by terminating the bus waveguide at an appropriate distance d from the drop channel entrance [see Fig. 3(c)]. In this way, not only the channel is open for the desired wavelength and closed for the other resonant wavelengths, but also the transmission efficiency is boosted; thanks to the coherent interference of back and forth waves. The transmission line model of the structure with the terminated bus waveguide is shown in Fig. 3(d). The terminated bus waveguide in this model is replaced by a transmission line loaded by a complex scalar impedance compliant with the Fresnel's law of reflection [5]:

$$Z_L = \sqrt{\varepsilon_d/\varepsilon_m} Z_d. \quad (9)$$

The coherent interference of waves at a certain wavelength requires that the length of the terminated bus be about a quarter of that wavelength. Obviously, at other wavelengths, the waves are no longer coherently adding up and thus, the transmission efficiency would reduce. The proposed model shows that $d = 230$ nm is an appropriate choice for the window centered at 800 nm. This is demonstrated in Fig. 4(b), where the results obtained by the proposed model and the COMSOL software virtually overlap with each other.

Now that the proposed model is validated, a two-channel demultiplexer is designed such that the transmission spectra of the first and second drop channels have two windows with full width at half maximum of 50 nm at the infrared wavelengths 0.8 and 1 μ m. This structure is schematically shown in Fig. 5. First, the width of the waveguides is set to $W = 50$ nm and

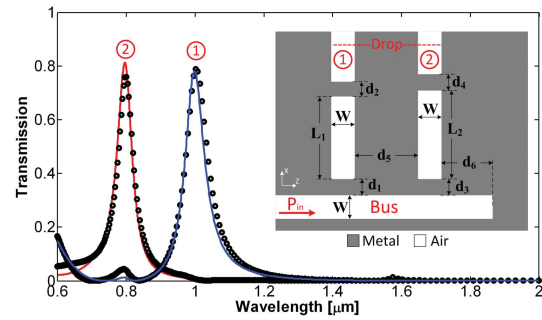


Fig. 5. Transmitted power spectra in the first and second drop channels of the designed two-channel demultiplexer shown in the inset of the figure.

then β_d , Z_d , β_m , and Z_m , are found at different wavelengths. The well-known techniques of microwave network analysis are then employed to find the geometrical dimensions of the structure: $L_1 = 300$ nm, $L_2 = 505$ nm, $d_1 = d_2 = d_3 = d_4 = 10$ nm and $d_6 = 230$ nm. The distance between the two channels (d_5) must be set such that we get a constructive interference of waves at the entrance of both channels. Since the difference between a quarter of wavelengths at 0.8 and 1 μ m is 50 nm, d_5 is expected to be around 50 nm. The exact value is however extracted from the model and is found to be about 60 nm. The transmitted power spectra of the first and second drop channels are extracted by using the proposed model (solid) and the COMSOL software (circles). The obtained results are plotted in Fig. 5. Once again, an excellent agreement is observed between the results.

In summary, we have proposed a strategy for modeling the evanescent coupling mechanism between MDM waveguides that can be used in analysis and design of any similar planar plasmonic structure, where direct- and side-coupling via evanescent wave tunneling are the operative factors. In particular, the proposed model is applicable to the plasmonic slot cavity structures reported in [9] and [10].

REFERENCES

- [1] L. Li, T. Li, S. Wang, S. Zhu, and X. Zhang, "Broad band focusing and demultiplexing of in-plane propagating surface plasmons," *Nano Lett.*, vol. 11, no. 10, pp. 4357–4361, 2011.
- [2] F. Hu, H. Yi, and Z. Zhou, "Wavelength demultiplexing structure based on arrayed plasmonic slot cavities," *Opt. Lett.*, vol. 36, no. 8, pp. 1500–1502, 2011.
- [3] G. Veronis and S. Fan, "Bends and splitters in metal-dielectric-metal subwavelength plasmonic waveguides," *Appl. Phys. Lett.*, vol. 87, no. 13, pp. 131102-1–131102-3, 2005.
- [4] H. Nejati and A. Beirami, "Theoretical analysis of the characteristic impedance in metal-insulator-metal plasmonic transmission lines," *Opt. Lett.*, vol. 37, no. 6, pp. 1050–1052, 2012.
- [5] A. Pannipitiya, I. Rukhlenko, and M. Premaratne, "Analytical modeling of resonant cavities for plasmonic-slot-waveguide junctions," *IEEE Photon. J.*, vol. 3, no. 2, pp. 220–233, Apr. 2011.
- [6] J. Liu, G. Fang, H. Zhao, Y. Zhang, and S. Liu, "Surface plasmon reflector based on serial stub structure," *Opt. Express*, vol. 17, no. 22, pp. 20134–20139, 2009.
- [7] H. Lu, X. Liu, D. Mao, Y. Gong, and G. Wang, "Induced transparency in nanoscale plasmonic resonator systems," *Opt. Lett.*, vol. 36, no. 16, pp. 3233–3235, 2011.
- [8] M. Rezaei, *et al.*, "A distributed circuit model for side-coupled nanoplasmonic structures with metal-insulator-metal arrangement," *IEEE J. Sel. Topics Quantum Electron.*, vol. 18, no. 6, pp. 1692–1699, Nov./Dec. 2012.
- [9] Y. Guo, *et al.*, "A plasmonic splitter based on slot cavity," *Opt. Express*, vol. 19, no. 15, pp. 13831–13838, 2011.
- [10] F. Hu, H. Yi, and Z. Zhou, "Band-pass plasmonic slot filter with band selection and spectrally splitting capabilities," *Opt. Express*, vol. 19, no. 6, pp. 4848–4855, 2011.